Passive Velocity Field Control (PVFC): Part II—Application to Contour Following

Perry Y. Li, *Member, IEEE* and Roberto Horowitz, *Member, IEEE*

***Abstract*—In contour following applications, the various degrees of freedom of a mechanical system have to be well coordinated, but very often, the speed at which the contour is followed is not critical. Moreover, in the context of machining, the system has to interact closely with its physical environment. When the contour following task is represented by a velocity field on the configuration manifold of the system, the coordination aspect of the problem is made explicit. The passive velocity field control (PVFC) scheme developed in the Part I companion paper [7] can then be applied to track the defined velocity field so that the desired contour is followed, and to ensure that the interaction of the closed-loop system with the physical environment is passive to enhance safety and stability. Unfortunately, for some contours, an encoding velocity field on the configuration manifold does not exist or is difficult to define and, as a consequence, the PVFC cannot be directly applied. For systems whose configuration manifolds are compact Lie groups and the desired contour is represented by a parameterized trajectory, a general methodology is developed, using a suspension technique, to define a velocity field on a manifold related to the configuration manifold of the system for which PVFC can be applied. With this strategy, timing along the contour can be naturally varied on-line by a *self-pacing* scheme so that the contour tracking performance can be improved. The experimental results for a 2 degree of freedom robot following a Lissajous contour illustrates and verifies the convergence and robustness properties of the PVFC methodology.**

***Index Terms*—Coordination, lie groups, passivity, self-pacing, suspension, velocity field.**

I. Introduction

THE manipulation task of a mechanical system is traditionally specified by means of a desired timed trajectory in the workspace. The control objective is to track this trajectory at every instant of time. In many contour following applications, the actual timing in the desired trajectory is unimportant compared to the coordination and synchronization requirement between the various degrees of freedom. For example, in machine deburring, the machine is required to traverse the contour at the maximum speed without exceeding the limits on the force experienced by the deburring tool. The requirement that the machine be at a position specified by a predetermined trajectory at each time may be an overly stringent imposition. Indeed, it has been demonstrated in [2], [11] that in the presence of uncertainties, trajectory based contour tracking algorithms tend to exhibit the radial reduction phenomenon where the radius of the actual contour is smaller than the desired one. Fig. 1 illustrates the situation.

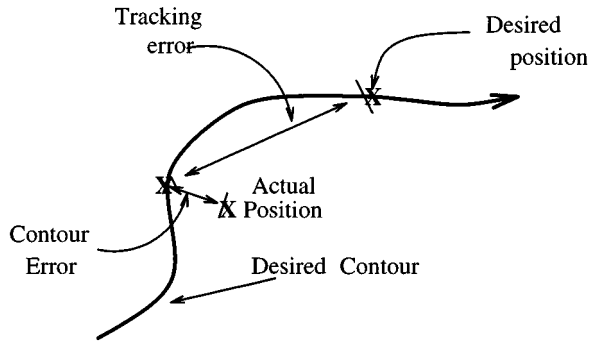

Fig. 1. In a timed trajectory based controller, the system may leave the desired contour to keep pace with the moving trajectory.

As an alternative, it is proposed in Part I of this paper [7] and in [6] that coordination critical tasks, such as contour following, can be encoded by a *time invariant* velocity field $V : \mathcal{G} \rightarrow T\mathcal{G}$ on the configuration space $\mathcal{G}$. An appropriately designed velocity field, which defines a desired velocity for each configuration of the mechanical system, guides the system to approach the contour in a well behaved manner.

To encode a contour following task, the velocity field should have the following properties:

i) its value at each point of the contour must be tangent to the contour;
ii) the flow of the field has a limit set which is contained in the contour.

Fig. 2 shows a velocity field for the task of tracing a circle on a rectangular configuration space. Notice that the flow of the field, which is determined by tracing the arrows, converges to the circle, and that the arrows are tangent to the circle.

Let $q(t) \in \mathcal{G}$ be the trajectory of the mechanical system. The velocity field tracking control objective is to cause the α-velocity field tracking error, $e_\alpha(t) := \dot{q}(t) - \alpha V(q(t))$ to vanish for some $\alpha > 0$, thus enabling the contour to be followed asymptotically. Notice that the mechanical system is not required to be at a particular position at each time. Instead, the velocity field guides the robot to approach the contour in a well behaved manner.

The passive velocity field control (PVFC) algorithm proposed in [5]–[7] ensures that a scaled multiple of the specified velocity field is asymptotically followed, i.e., $\dot{q}(t) \rightarrow \alpha V(q(t))$ for some $\alpha > 0$. In addition, when the feedback system is treated as an input–output system with the environment force F_e as its input, the velocity $\dot{q}$ as its output, and a supply rate

Manuscript received July 11, 1997; revised October 22, 2000 and June 23, 2001. Recommended by Associate Editor O. Egeland.

P. Y. Li is with the Department of Mechanical Engineering, University of Minnesota, Minneapolis MN 55455 USA (e-mail: pli@me.umn.edu).

R. Horowitz is with the Department of Mechanical Engineering, University of California at Berkeley, Berkeley CA 94720-1740 USA (e-mail: horowitz@me.berkeley.edu).

Publisher Item Identifier S 0018-9286(01)08826-2.

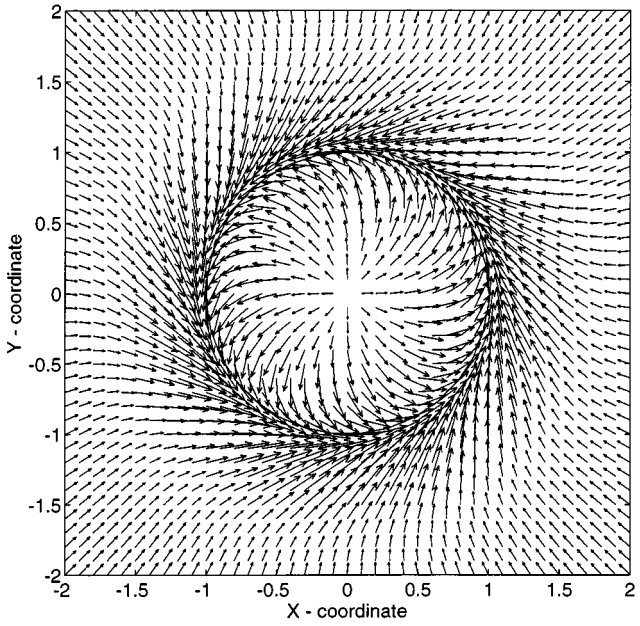

Fig. 2. A velocity field for the task of tracing a circle on a rectangular configuration space.

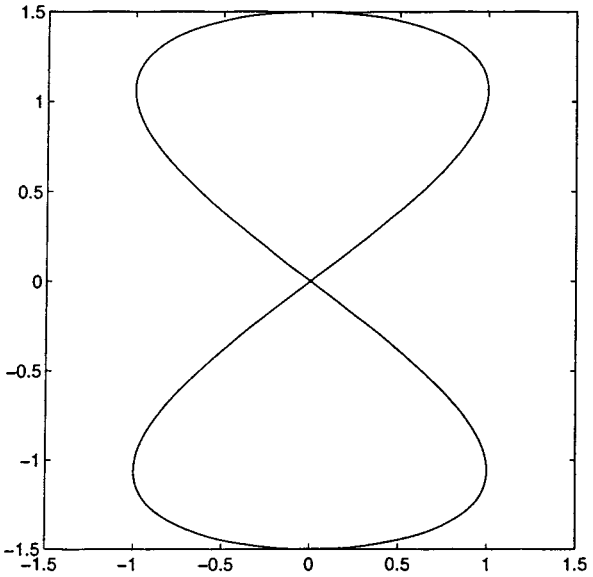

Fig. 3. Contour of the desired parameterized trajectory.

$s(F_e, \dot{q})$ defined to be the action of F_e on $\dot{q}$, $\langle F_e, \dot{q} \rangle$, which is the environment mechanical power input to the system, then the control scheme also maintains the passivity of the closed-loop system with respect to this supply rate in the sense that: for all $F_e(\cdot)$ and $t \geq 0$

$$\int_0^t s(F_e(\tau), \dot{q}(\tau)) d\tau \geq -c^2. \tag{1}$$

One advantage of maintaining passivity is that the coordination requirements of the contour following task becomes naturally embedded in the feedback system and will be decoupled from the speed at which the contour is followed. The speed, determined by the scalar α, is a function of the energy storage present in the feedback system. The latter can be controlled by a variety of additional control loops taking into account other environment factors, such as the magnitude of the interaction force. In the context of machining (e.g., cutting, deburring), where contour following problems are frequently encountered, the robot or the machine tool has to interact closely with its workpiece. If the closed-loop control system is passive with respect to the environment mechanical power, the energy in the system is limited to the initial energy of the system and the additional energy input from the environment. Since the physical environments with which the machine interacts are often passive themselves, stability and safety can be enhanced. For these reasons, the PVFC algorithm in [6], [7] is a good candidate for contour following applications.

In order to apply PVFC to contour following, a contour encoding velocity field must first be defined. Unfortunately, for many desired contours, such a velocity field is either difficult to define or may not even exist. The latter can happen when the tangent to the contour is not unique. For example, the center point of the Lissajous contour in Fig. 3 does not have a unique nonzero tangent and any velocity field must command the mechanical system to stop at the intersection.

In this paper, this difficulty is overcome by using a parameterized trajectory description of the contour. A parameterized trajectory is a curve $x_d : \mathcal{I} \rightarrow \mathcal{G}$ where $\mathcal{I} \subset \Re$ and $\mathcal{G}$ is the configuration space of the mechanical system. It reduces to the traditional desired trajectory if $\mathcal{I}$ is time. A suspended system is then defined so that the configuration $q(t)$ of the mechanical system and the parameterization $\tau(t) \in \mathcal{I}$ of the contour are coordinated. This is achieved by defining a *time invariant* velocity field on the suspended configuration space $\overline{\mathcal{G}} := \mathcal{G} \times \mathcal{I}$ using the concepts of gradient vector fields [4] and *self-pacing*. The basic idea behind *self-pacing* is to increase or decrease the desired rate of the progression of the parameter τ relative to the desired speed of the mechanical system, based on the deviation of the configuration q from the desired location $x_d(\tau)$. The general procedure for the design of such a velocity field will be developed for mechanical systems with compact Lie groups as their configuration spaces. These constitute a wide class of important mechanical control systems including revolute jointed manipulators, satellites, and underwater vehicles. Under the same assumption, we show that the mechanical system converges to the parameterized trajectory. Extensive experiments have been conducted for a 2-link revolute jointed serial robot following the Lissajous figure in Fig. 3 to validate the proposed method and to illustrate the convergence and robustness properties of the PVFC as presented in [7].

The rest of this paper is organized as follows: in Section II, we briefly review the PVFC algorithm and its properties, which are developed in detail in [6], [7]. In Sections III–IV, we constructively show that a contour following problem in which the contour is described by a parameterized curve reduces to the velocity field following problem, so that PVFC can be applied. In Section III, this procedure is performed for a 2 DOF SCARA robot whose configuration space is the 2-torus, $\mathcal{T}^2$, to illustrate the method. In Section IV, the procedure is generalized to mechanical systems with compact Lie groups as their configuration

spaces, and the main convergence results are also presented. Experimental results are given in Section V. Section VI contains concluding remarks.

Throughout the paper, unbold letters or symbols denote elements in a manifold, respective bold letters and symbols denote their coordinate representations. Thus, the coordinate representation of $v \in T\mathcal{G}$ is $\mathbf{v} = [v^1, v^2, \ldots, v^n]^{\mathrm{T}}$ so that $v = \sum_{i=1}^{n} v^i \partial/\partial q^i$, where $\partial/\partial q^i$ are the coordinate basis vectors. $\langle F, v\rangle$ denotes the action of the co-vector (or 1-form) F on the tangent vector (or a vector field) v. $\langle\langle v, w\rangle\rangle$ denotes the inner product defined by some Riemannian metric (sometimes with subscripts to signify the inertia metric that defines it).

II. Review of Passive Velocity Field Control (PVFC)

In this section, we briefly review and summarize the design procedure for and properties of PVFC. The readers are referred to [6], [7] for details.

We consider a n-degree of freedom fully actuated mechanical system with configuration space $\mathcal{G}$ subject to both control forces T and environment forces F_e. Its dynamics can be expressed geometrically in terms of a Levi–Civita connection [7]

$$M\nabla_{\dot{q}}\dot{q} = T + F_e \tag{2}$$

or in terms of coordinates as

$$\mathbf{M}(\mathbf{q})\ddot{\mathbf{q}} + \mathbf{C}(\mathbf{q}, \dot{\mathbf{q}})\dot{\mathbf{q}} = \mathbf{T} + \mathbf{F}_e \tag{3}$$

where ∇ is the Levi–Civita connection associated with the inertia metric M, $\mathbf{M}(\mathbf{q})$ and $\mathbf{C}(\mathbf{q}, \dot{\mathbf{q}})$ are the inertia matrix and Coriolis matrix in coordinates.

Given $V : \mathcal{G} \to T\mathcal{G}$, the desired velocity field that the system is supposed to track, the design methodology presented in [7] consists in the following three steps.

1) Defining an augmented system as a product system with configuration space $\mathcal{G}_a = \mathcal{G} \times S^1$, between the plant (2) and a fictitious flywheel

$$M^a \nabla^a_{\dot{q}_a} \dot{q}_a = \begin{pmatrix} M\nabla_{\dot{q}}\dot{q} \\ M_f \ddot{q}^{n+1} \end{pmatrix} = \underbrace{\begin{pmatrix} T \\ T_{n+1} \end{pmatrix}}_{T^a} + \underbrace{\begin{pmatrix} F_e \\ 0 \end{pmatrix}}_{F_e^a} \tag{4}$$

where $q_a = (q, q^{n+1})$ and M^a are the configuration and the inertia Riemannian metric on $\mathcal{G}_a$ for the augmented system. In coordinates, the latter is given by $\mathbf{M}^a(\mathbf{q}) = \mathrm{diag}(\mathbf{M}(\mathbf{q}), \mathrm{M_f}) \in \Re^{(n+1)\times(n+1)}$. M^a defines the kinetic energy of the augmented system via:

$$\kappa_a(\dot{q}_a) = \langle\langle \dot{q}_a, \dot{q}_a \rangle\rangle_a = \frac{1}{2}\dot{\mathbf{q}}_a^{\mathrm{T}} \mathbf{M}^a(\mathbf{q}_a)\dot{\mathbf{q}}_a \tag{5}$$

where $\langle\langle \cdot, \cdot \rangle\rangle_a$ denotes the inner products defined by the inertia metric M^a.

2) Defining an augmented desired velocity field of the form: $V^a(q_a) = (V(q), V^{n+1}(q)) \in T\mathcal{G}_a$, such that the kinetic energy of the augmented system is a constant

$$\kappa_a(V_a) = \frac{1}{2}\mathbf{V}^{\mathrm{T}}(\mathbf{q})\mathbf{M}(\mathbf{q})\mathbf{V}(\mathbf{q}) + \frac{1}{2}M_f\left(V^{n+1}\right)^2 = \overline{E}. \tag{6}$$

3) Defining a coupling control T^a in (4) of the form

$$\begin{aligned} T^a &= \dot{q}_a \rfloor \Omega_t(q_a); \\ \mathbf{T}^a &= \mathbf{G}(\mathbf{q}_a, \dot{\mathbf{q}}_a)\dot{\mathbf{q}}_a + \gamma \mathbf{R}(\mathbf{q}_a, \dot{\mathbf{q}}_a)\dot{\mathbf{q}}_a \end{aligned} \tag{7}$$

where

γ	gain constant;
Ω_t	time varying two-form;
$\rfloor$	contraction operator;
$\mathbf{G}(\mathbf{q}_a, \dot{\mathbf{q}}_a)$ and $\mathbf{R}(\mathbf{q}_a, \dot{\mathbf{q}}_a)$	skew-symmetric matrices.

Ω_t, $\mathbf{G}(\mathbf{q}_a, \dot{\mathbf{q}}_a)$ and $\mathbf{R}(\mathbf{q}_a, \dot{\mathbf{q}}_a)$ depend on the augmented velocity field $V_a(q_a)$. Their exact definitions can be found in [6] and [7]The closed-loop system consisting of the augmented system (4) and the coupling control (7), is given by

$$M^a \nabla^{c,\gamma}_{\dot{q}_a} \dot{q}_a = F_e^a. \tag{8}$$

The key passivity and convergence properties of PVFC are summarized below:

Theorem 1[6], [7]: The closed-loop system (8) consisting of the augmented system (4) and the coupling control (7) has the following properties.

1) The closed-loop affine connection $\nabla^{c,\gamma}$ is compatible with the augmented inertia metric M^a so that the kinetic energy of the augmented system κ_a in (5) satisfies

$$\frac{d}{dt}\kappa_a(\dot{q}_a(t)) = \langle T_e, \dot{q}\rangle = \mathbf{T}_e{}^{\mathrm{T}}(t)\dot{\mathbf{q}}(t). \tag{9}$$

2) The controlled system is passive with respect to the supply rate $s(F_e, \dot{q}) = \langle T_e, \dot{q}\rangle = \mathbf{T}_e^{\mathrm{T}}\dot{\mathbf{q}}$.
3) For each $\alpha \in \Re$, define the α-velocity field error to be $e_\alpha := \dot{q}_a - V_a(q_a)$. Then, as long as $\gamma\ \alpha \geq 0$ where γ is the feedback gain in (7), $\mathbf{e}_\alpha = \mathbf{0}$ is a Lyapunov stable solution if $F_e \equiv 0$, i.e., in the absence of environment forces.
4) Let $\beta(t)$ be related to the kinetic energy of the system via:

$$\beta(t) = \mathrm{sign}(\gamma)\sqrt{\frac{\kappa_a(\dot{q}_a(t))}{\overline{E}}}. \tag{10}$$

Therefore, because of (9), $\beta(t) = \beta(0) = \beta$ when $F_e \equiv 0$. In this case, we also have

$$\dot{q}_a \to \beta V_a(q_a), \text{ and } \dot{q} \to \beta V(q), \tag{11}$$

globally and exponentially, except from a set of initial conditions of measure 0.

Remark 1: The exponential velocity field convergence property is established using the following Lyapunov function, which will be useful for establishing the contour following convergence result in Section IV:

$$W_\beta(t) := \frac{1}{2}\langle\langle e_\beta, e_\beta\rangle\rangle_a = \frac{1}{2}\mathbf{e}_\beta^{\mathrm{T}}(t)\mathbf{M}^a(\mathbf{q}_a(t))\mathbf{e}_\beta(t) \tag{12}$$

where $e_\beta(t) = \dot{q}_a(t) - \beta(t)V_a(q_a(t))$. $W_\beta(t)$ satisfies

$$\dot{W}_\beta(t) = -4\overline{E}\gamma\beta\mu(t)W_\beta(t), \tag{13}$$

where $\mu(t) \geq 0$ is a nondecreasing function, and $\mu(0) = 0$ if and only if $\dot{q}_a(0) = -\mathrm{sign}(\gamma)\beta V_a(q_a(0))$. Therefore, the

rate of convergence is given by $2\gamma\beta\overline{E}$ in the neighborhood of $e_\beta = 0$.

In addition, the PVFC has the following robustness properties, which shall be verified from the experimental results in Section V. The readers are referred to the companion paper [7] for details.

1) If the environment force is in the direction $F_e^a = \delta(t)P^a$, where $P^a = M^a V_a$ is the desired momentum and $\delta(t) \in \Re$, then its effects on the velocity field tracking error given by $e_\beta := \dot{q}_a - \beta(t)V_a(q_a(t))$ with β defined in (10), can be eliminated if the feedback gain γ is sufficiently large.
2) If the environment force is in the direction that annihilates V_a, i.e., $\langle F_e^a, V_a\rangle = 0$, then the velocity tracking error e_β will be ultimately bounded.
3) As the energy of the system increases (i.e., $\beta(t)$ increases), the lower bound for the gain γ needed in 1) as well as the ultimate bound in 2) both decrease. Thus, we expect that the performance of the system to improve as the speed of the system is increased.

III. Applying PVFC to Contour Following: An Illustrative Example in $\mathcal{T}^2$

In this and the next sections, we discuss the application of PVFC to contour following problems. Since the design of a contour encoding velocity field may be difficult and for some contours impossible, we develop a general methodology to achieve contour following by representing the contour as a parameterized trajectory, instead of just a set of points. A parameterized trajectory is a curve $x_d : \mathcal{I} \to \mathcal{G}$ where $\mathcal{I} \subset \Re$ and $\mathcal{G}$ is the configuration space of the manipulator. If $\mathcal{I}$ is time, then the parameterized trajectory reduces to the traditional desired trajectory.

The key ideas are to i) dynamically extend the mechanical system to include the parameter τ of the parameterized trajectory as another coordinate, forming a *suspended* system; ii) design a velocity field on the suspended system configuration space in order to require that the mechanical system and the parameter τ are coordinated; iii) apply the PVFC methodology to the suspended system. Following [4], the velocity field will be designed so as to be related to a gradient vector field of a potential function.

To illustrate the procedure, we first consider the two-link manipulator in Fig. 4 where $\mathcal{G}$ is the torus $\mathcal{T}^2$, identified with $[0, 2\pi) \times [0, 2\pi)$. Hence, the joint angles $\mathbf{q} = (q^1, q^2)^{\mathrm{T}}$ in Fig. 4 will be the coordinates of the system. The more general case where the configuration manifold is a compact Lie group will be presented in Section IV.

A. Suspension

First, we form a suspended system by forming a product system from the original dynamical system and the dynamics of the evolution of the parameterization $\tau \in \mathcal{I}$:

$$\begin{pmatrix} \mathbf{M}(\mathbf{q}) & \mathbf{0}_{n\times 1} \\ \mathbf{0}_{1\times n} & 1 \end{pmatrix} \begin{pmatrix} \ddot{\mathbf{q}} \\ \ddot{\tau} \end{pmatrix} + \begin{pmatrix} \mathbf{C}(\mathbf{q}, \dot{\mathbf{q}})\dot{\mathbf{q}} \\ 0 \end{pmatrix} = \begin{pmatrix} \mathbf{T} \\ T_\tau \end{pmatrix} + \begin{pmatrix} \mathbf{F}_e \\ 0 \end{pmatrix} \tag{14}$$

where the first row in (14) corresponds to the dynamics of the two link robot with $\mathbf{q} \in \Re^2$ being the coordinates, $\mathbf{M}(\mathbf{q}) \in \Re^{2\times 2}$ being the inertia matrix, $\mathbf{C}(\mathbf{q}, \dot{\mathbf{q}}) \in \Re^{2\times 2}$ being the Coriolis matrix, $\mathbf{T} \in \Re^2$ represents the control forces, and $\mathbf{F}_e \in \Re^2$ represents the environment forces.

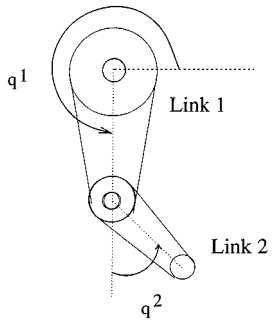

Fig. 4. A two link direct drive robot.

The suspended system (14) corresponds to a mechanical system with configuration $\overline{\mathbf{q}} = \begin{pmatrix} \mathbf{q} \\ \tau \end{pmatrix}$ and inertia and Coriolis matrices

$$\overline{\mathbf{M}}(\overline{\mathbf{q}}) = \begin{pmatrix} \mathbf{M}(\mathbf{q}) & 0 \\ 0 & 1 \end{pmatrix}, \quad \overline{\mathbf{C}}(\overline{\mathbf{q}}, \dot{\overline{\mathbf{q}}}) = \begin{pmatrix} \mathbf{C}(\mathbf{q}, \dot{\mathbf{q}}) & \mathbf{0}_{n\times 1} \\ \mathbf{0}_{1\times n} & 0 \end{pmatrix}$$

under the influence of the environment force $\overline{\mathbf{F}}_e = \begin{pmatrix} \mathbf{F}_e \\ 0 \end{pmatrix}$ and control torque $\overline{\mathbf{T}} = \begin{pmatrix} \mathbf{T} \\ T_\tau \end{pmatrix}$. Equation (14) can be written as

$$\overline{\mathbf{M}}(\overline{\mathbf{q}})\ddot{\overline{\mathbf{q}}} + \overline{\mathbf{C}}(\overline{\mathbf{q}}, \dot{\overline{\mathbf{q}}})\dot{\overline{\mathbf{q}}} = \overline{\mathbf{T}} + \overline{\mathbf{F}}_e. \tag{15}$$

The next steps will be 1) to define a suitable velocity field for the suspended mechanical system that encodes the contour following task, and 2) to apply PVFC to ensure that this velocity field is tracked. Thus, PVFC will control the dynamics of both the mechanical system itself and of the parameterization τ.

B. Velocity Field Design on $\mathcal{T}^2 \times \mathcal{I}$

It is now necessary to design a velocity field on $\overline{\mathcal{G}} = \mathcal{G} \times \mathcal{I}$, the configuration space of the suspended system in (15), given a parameterized trajectory $x_d : \mathcal{I} \to \mathcal{G}$. Using the joint angles as coordinates, let $\mathbf{x}_d(\tau) = [x_d^1(\tau), x_d^2(\tau)]^{\mathrm{T}}$ be the desired parameterized trajectory in these coordinates. Define the angle error function $\mathbf{E} : \mathcal{T}^2 \times \mathcal{I} \to \mathcal{T}^2$ to be

$$\mathbf{E}(\mathbf{q}, \tau) := \begin{pmatrix} E^1(\mathbf{q}, \tau) \\ E^2(\mathbf{q}, \tau) \end{pmatrix} := \begin{pmatrix} \left(q^1 - x_d^1(\tau)\right) \bmod 2\pi \\ \left(q^2 - x_d^2(\tau)\right) \bmod 2\pi \end{pmatrix}. \tag{16}$$

Next, we define a potential function $U : \mathcal{T}^2 \to \Re$ by

$$U(\mathbf{E}) := \frac{1}{2}\left[h_1(1 - \cos(E^1)) + h_2(1 - \cos(E^2))\right] \tag{17}$$

where h_1, h_2 are positive constants, and E^i is the ith component of $\mathbf{E}$. Notice that U attains its minimum when $\cos(E^1) = \cos(E^2) = 1$ and increases as $\mathbf{q}$ deviates more from the desired location $\mathbf{x}_d(\tau)$. Thus, $U(E)$ is a measure of the tracking performance.

The velocity field $\mathbf{V}$ on $\overline{\mathcal{G}}$ is defined to be a linear combination of two terms as follows:

$$\mathbf{V}(\overline{\mathbf{q}}) := \begin{pmatrix} V^1 \\ V^2 \\ V_{\mathcal{I}} \end{pmatrix} = \lambda_1(\overline{\mathbf{q}}) \begin{pmatrix} \frac{dx_d^1}{d\tau}(\tau) \\ \frac{dx_d^2}{d\tau}(\tau) \\ 1 \end{pmatrix} - \lambda_2(\overline{\mathbf{q}}) \begin{pmatrix} h_1 \sin E^1 \\ h_2 \sin E^2 \\ 0 \end{pmatrix} \tag{18}$$

where $\lambda_1, \lambda_2 : \overline{\mathcal{G}} \to \Re^+$ are positive bounded functions. The rationales for this definition of $\mathbf{V}$ in (18) are as follows.

- The first term in (18) satisfies

$$\begin{pmatrix} \frac{\partial E^1}{\partial q^1} & \frac{\partial E^1}{\partial q^2} & \frac{\partial E^1}{\partial \tau} \\ \frac{\partial E^2}{\partial q^1} & \frac{\partial E^2}{\partial q^2} & \frac{\partial E^2}{\partial \tau} \end{pmatrix} \left\{ \lambda_1(\overline{\mathbf{q}}) \begin{pmatrix} \frac{dx_d^1}{d\tau}(\tau) \\ \frac{dx_d^2}{d\tau}(\tau) \\ 1 \end{pmatrix} \right\} = \begin{pmatrix} 0 \\ 0 \end{pmatrix}.$$

  Therefore, it is a precompensation term coordinating the dynamics of $\mathbf{q}$ and τ so that if $\dot{\overline{\mathbf{q}}}$ of the suspended system (15) is in this direction, $\mathbf{E}(\overline{\mathbf{q}}(t))$ will remain unchanged.
- For the second term, notice that the $\partial/\partial q^1$ and $\partial/\partial q^2$ components are in fact

$$\begin{pmatrix} \frac{\partial U}{\partial E^1} \\ \frac{\partial U}{\partial E^2} \end{pmatrix} = \begin{pmatrix} h_1 \sin(E^1) \\ h_2 \sin(E^2) \end{pmatrix}$$

  which can be shown to be the gradient vector field for an appropriate metric on $\mathcal{T}^2$. Indeed, if the direction of $\dot{\overline{\mathbf{q}}}$ is opposite to it

$$\frac{d}{dt}U(E(t)) = -\lambda_2(\overline{\mathbf{q}}) \left\{ \left(\frac{\partial U}{\partial E^1} \right)^2 + \left(\frac{\partial U}{\partial E^2} \right)^2 \right\} \leq 0.$$

- The combined effect of the two terms in (18) is that if $\dot{\overline{\mathbf{q}}} = \beta \mathbf{V}$ for some $\beta > 0$ (as expected from (11) in Theorem 1), then

$$\dot{\mathbf{E}} = -\beta \lambda_2(\overline{\mathbf{q}}) \begin{pmatrix} \frac{\partial U}{\partial E^1} \\ \frac{\partial U}{\partial E^2} \end{pmatrix} \tag{19}$$

  so that

$$\frac{d}{dt}U(E(t)) = -\beta \lambda_2(\overline{\mathbf{q}}) \left\{ \left(\frac{\partial U}{\partial E^1} \right)^2 + \left(\frac{\partial U}{\partial E^2} \right)^2 \right\} \leq 0. \tag{20}$$

Because $U(E)$ is lower bounded, (20) implies that $U(E(t))$ converges. The potential function $U(\mathbf{E})$ in (17) ensures that, as long as $\beta\lambda_2(\overline{\mathbf{q}})$ is uniformly positive, $\mathbf{E}$ must converge to a critical point of U, which are characterized by $E^i = 0$ or π, $i = 1, 2$. However, since the only stable critical point is $E^1 = E^2 = 0$, $\dot{\overline{\mathbf{q}}} = \beta\mathbf{V}$ implies that $\mathbf{q}(t) \to \mathbf{x}_d(\tau(t))$ from almost anywhere.

Once a velocity field on $\mathcal{G} \times \mathcal{I}$ is designed, the PVFC machinery summarized in Section II can be applied to the **suspended system** in (15) to track the velocity field (18). Since the passive velocity field controller involves augmenting the system to be controlled by the dynamics of a fictitious flywheel with configuration space S^1, the configuration space of such an augmented system becomes $\mathcal{G}_a = \bar{\mathcal{G}} \times S^1 = \mathcal{G} \times \mathcal{I} \times S^1$. The overall controller will now have 3 internal states: $\tau, \dot{\tau}$, and the fictitious flywheel velocity. $\dot{q}^{n+1}$. Notice that the flywheel configuration itself, q^{n+1}, is not needed (see [6], [7] for details).

C. Self-Pacing

Notice that (19) is independent of $\lambda_1(\overline{\mathbf{q}})$. However, it would take some time for the angle error $\mathbf{E}$ to decrease to an acceptable level. If the speed of the progression parameter $\dot{\tau}$ is large, a large portion of the contour will be tracked poorly. We can decrease this portion by decreasing $\dot{\tau}$. In general, the relative magnitudes of $\lambda_1(\overline{\mathbf{q}})$ and $\lambda_2(\overline{\mathbf{q}})$ control the speed of progression of the desired parameterized contour relative to the rate of convergence.

The idea of *self-pacing* is to exploit this relationship to improve contour following performance. One possibility is to make $\lambda_1(\overline{\mathbf{q}})$ and $\lambda_2(\overline{\mathbf{q}})$ depend on the value of the potential function $U(\mathbf{E}(\mathbf{q}, \tau))$ in (17), which measures the deviation of the configuration from the desired location, so that the velocity field emphasizes the action that decreases the tracking error when $U(\mathbf{E})$ is large. Consequently, when the tracking error is large, the desired trajectory $\mathbf{x}_d$ would progress at a slower speed. For example, $\lambda_1(\overline{\mathbf{q}}), \lambda_2(\overline{\mathbf{q}})$ can be:

$$\begin{aligned} \lambda_1(\overline{\mathbf{q}}) &= \exp(-R \cdot U(E(q, \tau))) \\ \lambda_2(\overline{\mathbf{q}}) &= 2 - \exp(-R \cdot U(E(q, \tau))) \end{aligned} \tag{21}$$

where $R > 0$ is the self-pacing parameter such that as R increases, the emphasis on eliminating contour following error is also increased.

The experimental results of this control scheme are presented in Section V.

IV. General Case Where $\mathcal{G}$ Is a Compact Lie Group

In this section, we generalize the procedure of applying PVFC to contour following problem, given in Section III to the generic setting when the configuration space is a compact Lie Group. The design procedure for the velocity field is motivated by the navigation function approach to real-time path planning introduced in [4].

Before we proceed, let us recall some differential geometric concepts and notations.

A smooth manifold $\mathcal{G}$ is a Lie Group if it has a group structure. Specifically, there exist 1) a smooth group operation $\cdot : (q_1, q_2) \mapsto q_1 \cdot q_2 \in \mathcal{G}$, 2) an identity element $id \in \mathcal{G}$ such that $q \cdot id = id \cdot q = q \; \forall q \in \mathcal{G}$, and 3) a smooth inverse operator denoted by $q \mapsto q^{-1} \in G$ such that $q \cdot q^{-1} = q^{-1} \cdot q = id$.

The group operator defines a family of left and right translation operators. For $a \in \mathcal{G}$, the *left translation by* a is denoted by $L_a : \mathcal{G} \to \mathcal{G}$, $L_a b = a \cdot b$, and the *right translation by* a is denoted by $R_a : \mathcal{G} \to \mathcal{G}$, $R_a b = b \cdot a$. Hence, $L_a b = R_b a = a \cdot b$.

Let $f : \mathcal{M} \to \mathcal{N}$, the *push forward* of f, denoted by $f_* : T\mathcal{M} \to T\mathcal{N}$ maps a tangent vector at $m \in \mathcal{M}$ to a tangent vector at $f(m) \in \mathcal{N}$ such that if $g : \mathcal{N} \to \Re$, $\mathcal{L}_{f_* v_m} g = \mathcal{L}_{v_m}(g \circ f)$, where $\mathcal{L}_v s$ denotes the Lie (directional) derivative of $s : \mathcal{M} \to \Re$ in the direction $v \in T\mathcal{M}$.

Let $g : \mathcal{G} \to \Re$, we shall use the notation, $\mathbf{d}\, g$ to denote the 1-form such that for all $v \in T\mathcal{G}$, the action of $\mathbf{d}\, g$ on v is $\langle \mathbf{d}\, g, v \rangle = \mathcal{L}_v g$.

Given $f : \mathcal{G} \to \Re$, and let $\langle\langle v, w \rangle\rangle$ be the inner products that define a Riemannian metric on $\mathcal{G}$. The *gradient vector field* $\mathrm{grad}\, f : \mathcal{G} \to T\mathcal{G}$ is defined by

$$\langle\langle \mathrm{grad}\, f, v \rangle\rangle = \langle \mathbf{d}\, f, v \rangle, \quad \forall v \in T\mathcal{G}.$$

A. Suspended System

The suspended system is formed in exactly the same way as in Section III, i.e.,

$$\begin{pmatrix} M\nabla_{\dot{q}}\dot{q} \\ \ddot{\tau} \end{pmatrix} = \begin{pmatrix} T \\ T_\tau \end{pmatrix} + \begin{pmatrix} F_e \\ 0 \end{pmatrix} \tag{22}$$

which can be rewritten as

$$\bar{M}\bar{\nabla}_{\dot{\bar{q}}}\dot{\bar{q}} = \bar{T} + \bar{F}_e. \tag{23}$$

where $\bar{q} = (q, \tau) \in \bar{\mathcal{G}} = \mathcal{G} \times \mathcal{I}$ is the configuration of the suspended system, $\bar{M}$ is its inertia metric, and $\bar{\nabla}$ is the Levi–Civita connection associated with $\bar{M}$. In coordinates, $\bar{M}$ is given by $\bar{\mathbf{M}}(\bar{\mathbf{q}}) = \mathrm{diag}(\mathbf{M}, 1)$, $\bar{T}$ and $\bar{F}_e$ are the control and environment forces for the suspended system.

B. Velocity Field Design

Assumption 1: The configuration space of the mechanical system is a compact Lie group, $\mathcal{G}$. The desired contour is defined by a parameterized curve $x_d : \mathcal{I} \to \mathcal{G}$ where $\mathcal{I} \subset \Re$ is the domain of the parameterization, and the derivative $(dx_d/d\tau)x_d : \mathcal{I} \to T\mathcal{G}$ is uniformly bounded.

The geometries of many robotic systems (see, for example, [8]) can be naturally described in terms of Lie Groups. $\mathcal{G}$ being compact can be considered equivalent to $\mathcal{G}$ being closed and bounded when embedded in R^p for some sufficiently large p. The assumption for $\mathcal{G}$ to be compact may be relaxed in many situations, as long as some of the boundedness conditions, which will become apparent, are satisfied.

To generalize the velocity field design procedure in Section III-B, we need to define

- a group error function $E(q, \tau) \in \mathcal{G}$;
- a potential function $U : E \mapsto \Re$ with the appropriate properties;
- a vector field on $\bar{\mathcal{G}}$ which leaves the error E invariant, corresponding to the first term in (18); and the gradient vector field of U, corresponding to the second term in (18).

1) Group Error Function and Navigation Function: Let $x_d : \mathcal{I} \to \mathcal{G}$, where $\mathcal{I} \subset \Re$, be the parameterized trajectory on a Lie group $\mathcal{G}$. Since $\mathcal{G}$ is a Lie group, a natural definition of the group error function is

$$E : \mathcal{G} \times \mathcal{I} \to \mathcal{G}, \quad E(q, \tau) := q \cdot x_d^{-1}(\tau) \in \mathcal{G}. \tag{24}$$

Similarly, one can choose to define $E(q, \tau) := x_d^{-1}(\tau) \cdot q$. However, the formulae given below will have to be properly adjusted.

Next, the potential function in (17) must be generalized. A function $U : \mathcal{G} \to \Re$ must be defined so that the flow of the gradient vector field of the function must converge to $id \in \mathcal{G}$, the identity from almost everywhere. Following [4], a *navigation function* as defined below possesses the sufficient conditions.

Definition 1: The twice differentiable function $U : \mathcal{G} \to \Re$ is a navigation function if it has the following properties:

1) all the critical points $(\{E_c \in \mathcal{G} : \mathbf{d}\, U(E_c) = 0\})$ are nondegenerate, i.e., the Hessian (which is the matrix of second derivatives) in any coordinate system, at each critical point has nonzero eigenvalues;
2) it has a unique minimum at the identity id with value 0.

Remark 2: The navigation function is defined so that all the critical points are isolated, and only the global minimum is stable. This together with the compactness of $\mathcal{G}$ ensures that the negative gradient flow of $U(\cdot)$ converges to a critical point, and to the global minimum from almost everywhere. A navigation function is in fact a Morse-Bott function [3] whose definition also requires that $U : \mathcal{G} \to \Re$ have compact sublevel sets. However, since $\mathcal{G}$ is assumed to be compact, this is automatic.

Examples:

1) For the control of satellite orientation, the configuration space of the satellite is $\mathcal{G} = SO(3)$, with each element q identified with a 3×3 real orthogonal matrix with determinant 1. The group action is the matrix multiplication and the identity element is the identity matrix, I. $T_q SO(3)$ can be identified with $\{q\,\omega \mid \omega \in so(3)\}$ where $so(3)$ is the space of 3×3 skew symmetric matrices. The error function can be defined to be

$$E(q, \tau) := q\, x_d^{-1}(\tau) = q\, x_d(\tau)^{\mathrm{T}} \tag{25}$$

where $x_d : \mathcal{I} \to SO(3)$ is the desired parameterized trajectory. Following [4], a navigation function over $SO(3)$ can be defined as follows. Let $P \in \Re^{3\times 3}$ be a symmetric matrix with distinct eigenvalues $\pi_1 < \pi_2 < \pi_3$ and $(\pi_1 + \pi_2)(\pi_1 + \pi_3)(\pi_3 + \pi_2) \neq 0$. The navigation function is defined to be

$$U(E) := \frac{1}{\pi'} \mathrm{tr} P(I - E) \tag{26}$$

where $\pi' = \pi_2 + \pi_3 - \pi_1$. Thus $E \in SO(3)$ is a critical point of $U(\cdot)$, iff

$$\mathrm{tr}\,(P\,E\,\omega) = 0 \quad \forall\, \omega \in so(3).$$

This is so iff PE is symmetric for which there are exactly four instances. Of these instances, it can be shown [1] that $E = I$ is the only critical point at which U has a positive definite Hessian (i.e., a minimum).

2) For revolute jointed robots, $\mathcal{G}$ is the n-torus $\mathcal{T}^n = S^1 \times \cdots \times S^1$ (n times), where S^1 is the circle. Each element of $\mathcal{T}^n$ can be identified with $q = (e^{jq^1}, \ldots, e^{jq^n})^{\mathrm{T}}$ where $q^i \in \Re$ is the angle of the ith joint and $j = \sqrt{-1}$. The identity element of $\mathcal{T}^n$ is $[1, \cdots, 1]^{\mathrm{T}}$ and the group action is given by

$$\begin{pmatrix} e^{jw^1} \\ \vdots \\ e^{jw^n} \end{pmatrix} \cdot \begin{pmatrix} e^{js^1} \\ \vdots \\ e^{js^n} \end{pmatrix} = \begin{pmatrix} e^{j(w^1+s^1)} \\ \vdots \\ e^{j(w^n+s^n)} \end{pmatrix}.$$

Let $\bar{q} = (q, \tau)$ with $q = (e^{jq^1}, \ldots, e^{jq^n})^{\mathrm{T}}$, and $x_d(\tau) = (e^{jx_d^1(\tau)}, \ldots, e^{jx_d^n(\tau)})^{\mathrm{T}}$ be the desired parameterized trajectory. The error function can be defined to be

$$E(\bar{q}) := \begin{pmatrix} e^{j\epsilon^1(\bar{q})} \\ \vdots \\ e^{j\epsilon^n(\bar{q})} \end{pmatrix}, \quad \epsilon^i = (q^i - x_d^i(\tau)). \tag{27}$$

Since $e^{j\cdot}$ is 2π periodic, it is equivalent to the error function in (16) when $n = 2$. A navigation function can be defined to be

$$U(E) := \sum_{i=1}^{n} h_i \left(1 - \cos(\epsilon^i)\right) \tag{28}$$

where $E = \left(e^{j\epsilon^1}, \ldots, e^{j\epsilon^n}\right)^{\mathrm{T}}$, and h_i's are positive constants.

The global minimum of $U(\cdot)$ is 0 and it corresponds to $E^i = 0$, for each i. Other critical points are characterized by $\sin(\epsilon^i) = 0$, $i = 1, \ldots, n$. The Hessians are given by the matrix $\mathrm{diag}(\cos(\epsilon^1), \ldots, \cos(\epsilon^n))$ so that it is positive definite iff ϵ^1, $\epsilon^2, \ldots, \epsilon^n$ are multiple of 2π, corresponding to the identity element which is also the global minimum.

2) Gradient Vector Field on $\overline{\mathcal{G}}$: We need to define a vector field $V : \overline{\mathcal{G}} \to T\overline{\mathcal{G}}$ such that

$$(E_* V)(\bar{q}) = \lambda_2(\bar{q}) \operatorname{grad} U(E(\bar{q}))$$

where E_* denotes the pushforward of the map $E : \overline{\mathcal{G}} \to \mathcal{G}$. To define a gradient vector field, a Riemannian metric is necessary. Let

$$\langle\langle \cdot, \cdot \rangle\rangle_V : T\overline{\mathcal{G}} \times T\overline{\mathcal{G}} \to \Re$$

be such a metric, which may not be related to the Riemannian metric that defines the inertia of the suspended system.

Lemma 1: Let $W(\bar{q}) = (W_{\mathcal{G}}(\bar{q}), W_{\mathcal{I}}(\bar{q}))$ be a vector field on $\overline{\mathcal{G}}$ where $\bar{q} = (q, \tau)$, $W_{\mathcal{G}}(\bar{q}) \in T_q\mathcal{G}$ and $W_{\mathcal{I}}(\bar{q}) \in T_\tau\mathcal{I}$. Then

$$E_* W(\bar{q}) = R_{\left[x_d^{-1}(\tau)\right]_*} \left[W_{\mathcal{G}}(\bar{q}) - \left(L_{E(\bar{q})}\right)_* \left((x_d)_* W_{\mathcal{I}}(\bar{q})\right)\right]$$

where E_* denotes the pushforward of the error function $E : \overline{\mathcal{G}} \to \mathcal{G}$, and $\left(L_{E(\bar{q})}\right)_*$, $(x_d)_*$, $\left(R_{x_d(\tau)}\right)_*$ denote the pushforward of the maps $L_{E(\bar{q})}$, x_d, and $R_{x_d(\tau)}$. L and R are, respectively, the left and right translation operators.

Proof: Let $W \in T_{\bar{q}}\overline{\mathcal{G}}$ be $W = (W_{\mathcal{G}}, W_{\mathcal{I}})$ where $\bar{q} = (q, \tau)$, $W_{\mathcal{G}} \in T_q\mathcal{G}$, and $W_{\mathcal{I}} = T_\tau\mathcal{I}$. Denote the inverse map by $\mathrm{inv} : \mathcal{G} \to \mathcal{G}, q \mapsto q^{-1}$. Notice that if $v \in T_q\mathcal{G}$

$$\mathrm{inv}_* v = -\left(L_{q^{-1}}\right)_* \circ \left(R_{q^{-1}}\right)_* v.$$

In matrix Lie groups, this is the familiar expression for $A \in \Re^{n \times n}$, $d(A^{-1}) = -A^{-1} dA A^{-1}$. Let us rewrite the error function in (24) as

$$E(\bar{q}) := q \cdot x_d^{-1}(\tau) = R_{x_d^{-1}(\tau)} q = L_q(x_d^{-1}(\tau)).$$

The push forward operator is essentially a derivative operator. Therefore, using the product rule on $E(\bar{q})$, we have

$$E_* W = \left(R_{x_d^{-1}(\tau)}\right)_* W_{\mathcal{G}} + (L_q \circ \mathrm{inv} \circ x_d)_* W_{\mathcal{I}}$$

where A_* denotes the pushforward of the map A. Expanding the expression for $E_* W$, we obtain

$$\begin{aligned} E_* W &= \left(R_{x_d^{-1}(\tau)}\right)_* W_{\mathcal{G}} + (L_q)_* \circ (\mathrm{inv})_* \circ (x_d)_* W_{\mathcal{I}} \\ &= \left(R_{x_d^{-1}(\tau)}\right)_* W_{\mathcal{G}} - (L_q)_* \circ \left(L_{x_d^{-1}(\tau)}\right)_* \\ &\quad \circ \left(R_{x_d^{-1}(\tau)}\right)_* \circ (x_d)_* W_{\mathcal{I}} \\ &= \left(R_{x_d^{-1}(\tau)}\right)_* \left[W_{\mathcal{G}} - \left(L_{q \cdot x_d^{-1}(\tau)}\right)_* \circ (x_d)_* W_{\mathcal{I}}\right] \\ &= \left(R_{x_d^{-1}(\tau)}\right)_* \left[W_{\mathcal{G}} - \left(L_{E(\bar{q})}\right)_* \circ (x_d)_* W_{\mathcal{I}}\right] \end{aligned} \tag{29}$$

which is the required result. In the above derivation, we used the fact that $(L_a)_* \circ (R_b)_* = (R_b)_* \circ (L_a)_*$, $(L_{a \cdot b})_* = (L_a)_* \circ (L_b)_*$, the formula for inv_* and $E(\bar{q}) = q \cdot x_d^{-1}(\tau)$. ■

Define the desired velocity field on $\bar{G} := \mathcal{G} \times \mathcal{I}$, $V = (V_{\mathcal{G}}, V_{\mathcal{I}})^{\mathrm{T}}$ where $V_{\mathcal{G}} \in T\mathcal{G}$ and $V_{\mathcal{I}} \in T\mathcal{I}$ for the parameterized trajectory $x_d : \mathcal{I} \to \mathcal{G}$ by

$$\begin{aligned} V(\bar{q}) &= \begin{pmatrix} V_{\mathcal{G}} \\ V_{\mathcal{I}} \end{pmatrix} \\ &= \lambda_1(\bar{q}) \begin{pmatrix} \left(L_{E(\bar{q})}\right)_* (x_d)_* 1_\tau \\ 1_\tau \end{pmatrix} \\ &\quad - \lambda_2(\bar{q}) \begin{pmatrix} \left(R_{x_d(\tau)}\right)_* \operatorname{grad} U(E(\bar{q})) \\ 0 \end{pmatrix} \\ \bar{q} &= (q, \tau) \end{aligned} \tag{30}$$

where $1_\tau \in T_\tau\mathcal{I}$ denotes a unit velocity vector and $\lambda_1(\bar{q})$ and $\lambda_2(\bar{q})$ are gain functions, defined so that

$$\overline{\lambda}_1 \geq \lambda_1(\bar{q}) > 0 \quad \overline{\lambda}_2 \geq \lambda_2(\bar{q}) \geq \epsilon > 0.$$

To enable *self-pacing*, $\lambda_1(\bar{q})$ and $\lambda_2(\bar{q})$ can be defined in the same way as in (21).

Proposition 1: Let $V = (V_{\mathcal{G}}, V_{\mathcal{I}})$ be the velocity field defined in (30), with $V_{\mathcal{G}}$ and $V_{\mathcal{I}}$ being the components in $T\mathcal{G}$ and in $T\mathcal{I}$ respectively, then for each $\bar{q} \in \overline{\mathcal{G}}$

$$(E_* V(\bar{q})) = -\lambda_2(\bar{q}) \operatorname{grad} U(E(\bar{q})). \tag{31}$$

Hence, if $\dot{\bar{q}} = V(\bar{q})$, $E(\bar{q}(t))$ evolves in the direction of the negative gradient field of $U(E)$, i.e.,

$$\frac{d}{dt} E(\bar{q}(t)) = -\lambda_2(\bar{q}) \operatorname{grad} U(E(\bar{q})).$$

Proof: This is a direct consequence of Lemma 1 applied to the velocity field in (30). ■

Examples:

1) Returning to the satellite orientation example where $\mathcal{G} = SO(3)$, let us define a Riemannian metric on $SO(3)$ as follows: let $q\omega_1, q\omega_2 \in T_q SO(3)$, where ω_1, ω_2 are 3×3 skew symmetric matrices

$$\langle\langle q\omega_1, q\omega_2 \rangle\rangle_V := \mathrm{tr}\left[\omega_1^{\mathrm{T}} \omega_2\right].$$

Let the error and navigation functions be defined as in (25), (26), and $\operatorname{grad} U(E) = E\omega$ where ω is a 3×3 skew-sym-

metric matrix to be determined. For any skew symmetric 3×3 matrix ζ

$$\operatorname{tr} \omega^{\mathrm{T}} \zeta = \langle \mathbf{d}\, U(E), E\zeta \rangle = -\frac{1}{\pi'} \operatorname{tr} PE\zeta.$$

From this and the fact that $\operatorname{tr} A\zeta = -\operatorname{tr} A^{\mathrm{T}}\zeta$, we obtain

$$\omega^{\mathrm{T}} = -\frac{PE - E^{\mathrm{T}}P}{2\pi'}$$

or

$$\operatorname{grad} U(E) = \frac{1}{2\pi'}(EPE - P).$$

Let $x_d(\tau) \in SO(3)$ be the desired parameterized trajectory. There exists $\Omega : \mathcal{I} \to so(3)$ so that

$$\frac{d}{d\tau} x_d(\tau) = x_d(\tau) \cdot \Omega(\tau).$$

The desired velocity field in (30) is then given by: $V : SO(3) \times \mathcal{I} \to TSO(3) \times T\mathcal{I}$

$$\begin{aligned} V(\bar{q}) =& \lambda_1(\bar{q}) \begin{pmatrix} E(\bar{q}) x_d(\tau) \Omega(\tau) \\ 1 \end{pmatrix} \\ & - \lambda_2(\bar{q}) \begin{pmatrix} \frac{1}{2\pi'}(EPE - P) x_d(\tau) \\ 0 \end{pmatrix} \\ =& \lambda_1(\bar{q}) \begin{pmatrix} q\Omega(\tau) \\ 1 \end{pmatrix} \\ & - \frac{\lambda_2(\bar{q})}{2\pi'} \begin{pmatrix} q\left[x_d(\tau)^{\mathrm{T}} P q - q^{\mathrm{T}} P x_d(\tau)\right] \\ 0 \end{pmatrix} \end{aligned}$$

since $E(\bar{q}) = q x_d^{\mathrm{T}}$.

2) Consider again the revolute jointed manipulator example where $\mathcal{G} = T^n$, the n-torus. Let $x_d(\tau) = \begin{pmatrix} e^{jx_d^1(\tau)} \\ \vdots \\ e^{jx_d^n(\tau)} \end{pmatrix}$ be the desired parameterized trajectory to be followed. Define the error function $E(\bar{q})$ and the navigation function $U(E)$ as in (27), (28). For each $q = \begin{pmatrix} e^{jq^1} \\ \vdots \\ e^{jq^n} \end{pmatrix}$, identify an element of $T_q\mathcal{G}$ by $\begin{pmatrix} e^{jq^1} v^1 \\ \vdots \\ e^{jq^n} v^n \end{pmatrix}$. Let the Riemannian metric on $\mathcal{G}$ be

$$\left\langle \left\langle \begin{pmatrix} e^{jq^1} v^1 \\ \vdots \\ e^{jq^n} v^n \end{pmatrix}, \begin{pmatrix} e^{jq^1} w^1 \\ \vdots \\ e^{jq^n} w^n \end{pmatrix} \right\rangle \right\rangle_V := \sum_i^n v^i w^i$$

which is the Euclidean metric. The velocity field on $\mathcal{G}$, $V(\bar{q})$ where $\bar{q} = (q, \tau)$ is given by: $\mathbf{V}(\bar{q}) = \begin{pmatrix} e^{jq^1 V^1(\bar{q})} \\ \vdots \\ e^{jq^n V^n(\bar{q})} \\ \lambda_1(\bar{q}) 1_\tau \end{pmatrix}$, where

$$V^i(\bar{q}) = \lambda_1(\bar{q}) \frac{dx_d^i}{d\tau} - \lambda_2(\bar{q}) h_i \sin E_i(\bar{q})$$

and $\lambda_1, \lambda_2 : \overline{\mathcal{G}} \to \Re^+$ are positive scalar bounded functions. ■

Remark 3: Obstacle avoidance can also be incorporated by defining suitable navigation functions. In this case, the navigation function should be defined such that its value is large at the locations of the obstacles, or the configuration space be punctured at those locations. Readers are referred to [9] and [10] for details of this approach.

C. PVFC Applied to the Suspended System

The PVFC summarized in Section II can now be applied to the $n+1$ degree of freedom (DOF) suspended system in (23) to track a multiple of the desired velocity field (30). The $n+2$ DOF closed-loop system that results has configuration space of $\mathcal{G}_a = \bar{\mathcal{G}} \times S^1$ after augmenting the $n+1$ DOF suspended system (23) by the fictitious flywheel, and incorporating the coupling control (7) (which depends on $V : \overline{\mathcal{G}} \to T\overline{\mathcal{G}}$ in (30)). Its dynamics will be given by (8) with the augmented inertia metric M^a given in coordinates by $\mathbf{M}^a(\mathbf{q}_a) = \operatorname{diag}(\bar{\mathbf{M}}, M_f)$ where $\bar{\mathbf{M}}(\bar{\mathbf{q}})$ is the inertia matrix for the suspended system, and M_f is the inertia of the fictitious flywheel.

The contour following result is given in the following theorem.

Theorem 2: Consider the closed-loop system (8) that results from the suspended system (23) under the control of the passive velocity field controller defined in Section II, and with the desired velocity field $V : \bar{\mathcal{G}} \to T\bar{\mathcal{G}}$ given by (30).

In the absence of environment force, i.e., $F_e \equiv 0$, the parameterized trajectory tracking error $E(\bar{q}(t))$ in (24) converges to one of the critical points of the navigation function $U(E)$. From almost every initial condition, $\dot{\bar{q}}(0) \in T\overline{\mathcal{G}}$, $E(\bar{q}(t))$ in fact converges to $id \in \mathcal{G}$, the identity element. Hence $q(t) \to x_d(\tau(t))$ from almost everywhere.

Asymptotically, the speed of the progression parameter is given by $\dot{\tau} = \beta \lambda_1(\bar{q})$, where $\beta = \operatorname{sign}(\gamma)\sqrt{\kappa_a(\dot{q}_a)/\overline{E}}$, $\kappa_a(\dot{q}_a)$ is the kinetic energy of the augmented system in (5), $\overline{E}$ is the constant used to construct the augmented velocity field V_a in (6), and $\lambda_1(\bar{q})$ is the gain parameter in (30).

Proof: We prove this theorem in a coordinate independent manner.

Let $\langle\langle \cdot, \cdot \rangle\rangle_a$ be the inner product defined by the augmented inertia metric M^a, and $\langle\langle \cdot, \cdot \rangle\rangle_V$ be the Riemannian metric on $\mathcal{G}$ used to compute the gradient vector field $\operatorname{grad} U(E)$. Further, define two types of norms on $T\mathcal{G}_a$, $\|e\|_a := \langle\langle e, e \rangle\rangle_a^{1/2}$, and $\|e\|_V := \langle\langle v, v \rangle\rangle_V^{1/2}$

First, recall from Theorem 1 that when $F_e \equiv 0$, $\beta(t) = \beta$ is a constant. Second, notice from the definition of the desired velocity field $V : \overline{\mathcal{G}} \to T\overline{\mathcal{G}}$ in (30) that the velocity of the error $E(q, \tau)$ is given by:

$$\dot{E}(\bar{q}(t)) = -\beta \lambda_2(\bar{q}) \cdot \operatorname{grad} U + (E \circ \pi_{\overline{\mathcal{G}}})_* e_\beta,$$

where $\bar{q} = (q, \tau)$, $\pi_{\overline{\mathcal{G}}} : \mathcal{G}_a \to \overline{\mathcal{G}}$ is the projection, and the second term is merely the component of $e_\beta \in T\mathcal{G}_a$ in $T\bar{\mathcal{G}}$

Now consider the Lyapunov function

$$\Omega(t) = \rho\, W_\beta(t) + U(E(\bar{q}(t))) \tag{32}$$

where W_β is defined in Remark 1, $U : \mathcal{G} \to \Re$ is the navigation function, and ρ is a positive number to be determined.Thus, from (13)

$$\frac{d}{dt}\Omega(t) = -\beta\{4\rho\overline{E}\gamma\mu(t)W_\beta(t) + \lambda_2(\bar{q}(t))\langle\langle \operatorname{grad} U(\bar{q}(t)), \operatorname{grad} U(\bar{q}(t))\rangle\rangle_V\} + \langle\langle \operatorname{grad} U(\bar{q}(t)), E_*\pi_{\overline{G}*}e_\beta\rangle\rangle_V. \quad (33)$$

Let k be the maximum of the induced norm of $(E \circ \pi_{\overline{G}})_*$, i.e., $\forall e \in T\mathcal{G}_a$,

$$k\|e\|_a \geq \|(E \circ \pi_{\overline{G}})_* e\|_a.$$

Notice that because $\mathcal{G}$ is assumed to be compact, k is finite. Then, (33) can be written as

$$\frac{d}{dt}\Omega \leq -\begin{pmatrix} \|\operatorname{grad} U\|_V, & \|e_\beta\|_a \end{pmatrix} \times \begin{pmatrix} \beta\lambda_2 & \frac{k}{2} \\ \frac{k}{2} & 2\rho\overline{E}\gamma\beta\mu(t) \end{pmatrix} \begin{pmatrix} \|\operatorname{grad} U\|_V \\ \|e_\beta\|_a \end{pmatrix}. \quad (34)$$

Hence, as long as $\gamma\beta > 0$ and $\mu(0) \neq 0$ (therefore, by Remark 1, $\mu(t) \geq \mu(0) > 0$), there is a $\rho > 0$ such that the matrix in (34) is positive–definite for all times. Using standard Barbalat's arguments (i.e., $\Omega(t)$ converges and $\dot{\Omega}(t)$ uniformly continuous, imply that $\dot{\Omega}(t) \to 0$), $\|e_\beta\|_a \to 0$ and $\|\operatorname{grad} U\|_V \to 0$.

If $U(E)$ has compact level sets (e.g., on a compact manifold), then $\operatorname{grad} U(E(t)) \to 0$ implies that E converges to one of the isolated critical point of U. However, since all the critical points except for $E = id$, the identity element of $\mathcal{G}$, are unstable, $E(\bar{q}(t)) \to id$, and $U(E(t)) \to 0$ from almost all initial conditions.

Finally, from (30), as $\operatorname{grad} U(E(t)) \to 0$, the $T\mathcal{I}$ component of the velocity field, $V(\bar{q}(t)) = \begin{pmatrix} V_\mathcal{G} \\ V_\mathcal{I} \end{pmatrix}$ is given by: $V_\mathcal{I}(\bar{q}(t)) \to \lambda_1(\bar{q}(t))1_\tau$. Since PVFC (Theorem 1) ensures that $\dot{\bar{q}} \to \beta V(\bar{q})$, we have $\dot{\tau} \to \beta V_\mathcal{I}(\bar{q}) \to \beta\lambda_1(\bar{q}(t))$. ■

Remark 4: Since $U(E)$ is a navigation function, its Hessian at $E = id$ is positive definite. There exists a neighborhood of $E = id$ and $\zeta > 0$

$$U(E) \leq \zeta\|\operatorname{grad} U(E)\|_V^2.$$

Thus, from (32) and (34), convergence of (E, e_β) to $(id, 0)$ is locally exponential, as long as β, which is determined by the kinetic energy of the augmented system, is nonzero.

Although we have restricted our attention to mechanical systems whose configuration spaces are compact Lie groups, the requirement for compactness can be replaced by other technical assumptions in certain cases. Specifically, we have used compactness in the following.

1) Compactness is used in conjunction with the definition of navigation functions to ensure that $\operatorname{grad} U(E(t)) \to 0$ implies that $E(t)$ converges to a critical point of $U(E)$. This condition can be satisfied if $U(E)$ is defined to have compact sublevel sets.
2) It is used to make sure that velocity field V defined in (30) is bounded when the gain functions $\lambda_1(\bar{q})$ and $\lambda_2(\bar{q})$ are uniformly bounded. Boundedness of V is necessary for the constant $\overline{E}$ in (6) to exist.
3) In the proof of Theorem 2, it is necessary that the induced norm of $(E \circ \pi_{\overline{G}})_* : T\mathcal{G}_a \to T\mathcal{G}$ is bounded. Many noncompact spaces, e.g., $\mathcal{G} = \Re^n$, satisfy this condition.

Therefore, compactness will not be necessary if these conditions can be independently guaranteed by other means, such as by the careful design of the navigation function. Similarly, the assumption that $\mathcal{G}$ has a group property may also be replaced if a meaningful alternate definition of group error function in (24) can be made, that is able to distinguish two different points in $\mathcal{G}$.

V. Experimental Results

The passive velocity field controller was applied to the 2 link direct drive SCARA manipulator in Fig. 4 to track a desired parameterized trajectory $q_d : \Re \to \mathcal{G}$, given by

$$x_d(\tau) = \begin{pmatrix} x_1^d(\tau) \\ x_2^d(\tau) \end{pmatrix} = \begin{pmatrix} \sin\left(\frac{2\pi}{3}\tau\right) \\ 1.5\cos\left(\frac{2\pi}{6}\tau\right) \end{pmatrix}, \quad \tau \in \Re.$$

The image of this parameterized trajectory is the Lissajous figure shown in Fig. 3. Notice that this trajectory is not one to one so that a time invariant velocity field on $\mathcal{G}$ that traces out the same contour does not exist.

For this parameterized trajectory, a velocity field on $\mathcal{G} \times \mathcal{I}$ was designed using (18) and (21), and the PVFC presented in Section II, with the fictitious flywheel velocity $M_f = 1$ in (4), was applied to the suspended system to track the extended velocity field as described previously.

A. Experimental Setup

Because of the existence of significant friction in the joints, a very simple friction compensation scheme was used in some of the experiments

$$F_1^{\text{comp}} = \text{fric}_1 \operatorname{sign}(\dot{\text{q}}^1); \quad \text{F}_2^{\text{comp}} = \text{fric}_2 \operatorname{sign}(\dot{\text{q}}^2) \quad (35)$$

where $\text{fric}_1 = 2.0$ Nm, $\text{fric}_2 = 3.0$ Nm. These terms were added to the T^a in (7).

In theory, when the passive velocity field controller is used, the total energy level in the system, $k_a(\dot{q}_a)$ in (5), should remain constant and the rate at which the parameterized trajectory progresses would be determined by the initial conditions. However, in actual implementations, dissipative forces and imperfect friction compensation can cause the energy level to vary. Thus, in order to control the nominal rate at which the parameterized trajectory progresses, in addition to the friction compensation in (35), the following exogenous signal was also added to T^a in (7)

$$T^{\text{forced}} = c \cdot P^a \cdot \left(r - \frac{\langle P^a, \dot{q}_a\rangle}{2\overline{E}}\right), \quad c > 0 \quad (36)$$

where $c = 0.01$ is a damping coefficient, and $P^a = M^a V_a \in T^*\mathcal{G}_a$ is the desired momentum of the augmented-suspended system. It can be shown that T^{forced} tends to cause the velocity $\dot{q}_a$ to stabilize at $r\ V_a$. In deburring applications, the nominal speed r can be made to depend on the measured force on the tool so that the maximum tool force is not exceeded.

The overall control scheme that combines the friction compensation, nominal speed control and the passive velocity field controller is shown in Fig. 5

B. Unforced Response

We first investigate the unforced response of the manipulator by setting $r = c = 0$ in (36). The initial value of the internal state of the controller (i.e., the fictitious flywheel velocity) was set to 10 and the manipulator was initially at rest. Thus, the initial total energy was 50. The self-pacing parameter in (21) was set to the nominal value $R = 100$. Notice that as the total energy of system dissipated, the manipulator was still able to follow the contour although the rate of traversal decreased (Fig. 6). However, the tracking performance as measured by the potential function $U(E)$ in (17) became progressively worse as the energy level decreased. This is consistent with the robustness result in [7] and summarized in Section II.

C. Effect of Self-Pacing

The effect of self-pacing on the response of the manipulator when the initial position of the manipulator is not on the desired contour is investigated next. As shown in Fig. 7, when $R = 0$ (no self-pacing), the manipulator approached from the initial position $(0, 0)$ to the desired contour by following a curved path. A controller that utilizes a time parameterized trajectory will also exhibit this behavior. When self-pacing was used $(R = 100)$, since the initial position error, and hence $U(E)$, was large, the parameter progressed slowed $(\dot{\tau} \approx 0)$ until the manipulator became close to the desired position $x_d(\tau)$. Hence, the robot approached the desired contour nearly in a straight line before moving along the contour.

The contour following performance at different self-pacing parameter values, (R) are shown in Fig. 8. In these experiments, the friction compensation scheme in (35) was in effect and r in (36) was kept at the nominal value of 1. In Fig. 8, the value of the potential function $U(E)$, which measures the tracking error, is plotted against the parameter τ during one pass of the contour. The desired contour repeated every 6τ coordinates units. Notice that the error was large at four distinct positions. These correspond to the regions when the joint velocities were required to reverse direction. Thus, stiction and friction are suspected to be the main cause of these errors. Notice also that as R in (21) was increased, $U(E)$ decreased. As expected, the improved performance was obtained at the expense of decreasing the rate at which the trajectory progressed at these critical regions along the contour.

D. Robustness to Friction

Since stiction/friction is suspected to be the main cause of the tracking error, it is interesting to investigate the performance of the control scheme when the friction compensation in (35) was removed. The tracking performances in this case at the different R values are shown in Fig. 9.

A comparison between Figs. 8 and 9 shows that tracking performance deteriorated when friction compensation was removed, as evidenced by the fact that at each value of R, $U(E)$ is approximately doubled when friction compensation is removed.

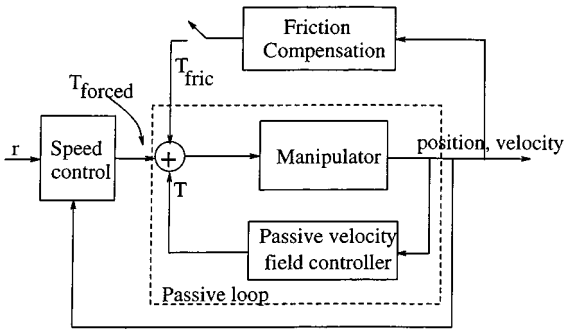

Fig. 5. Block diagram of control scheme.

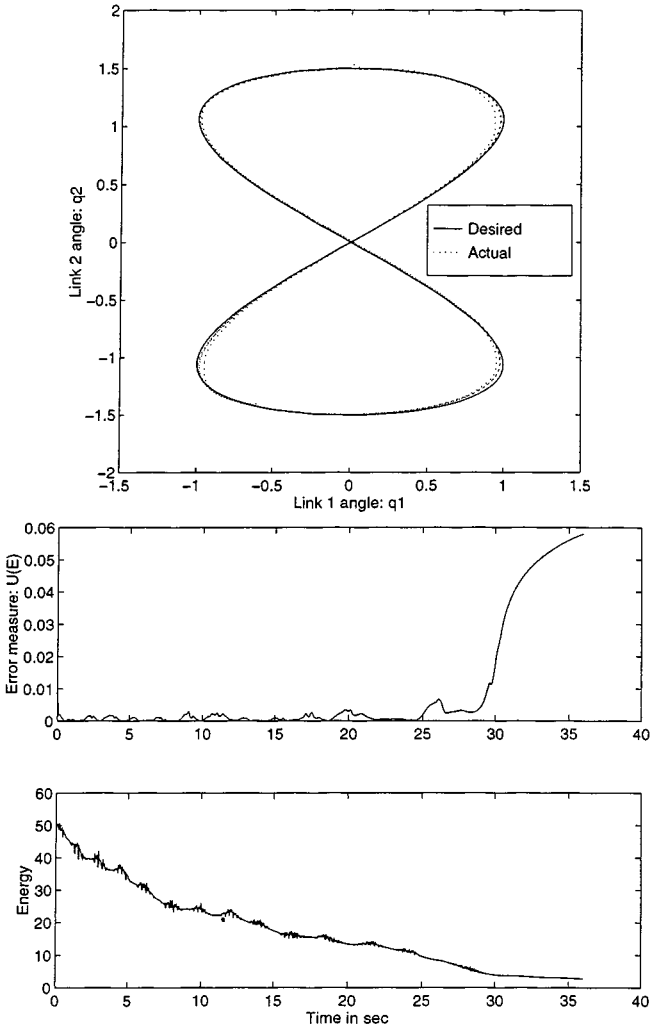

Fig. 6. Unforced response. Top: Contour traced. Middle: Value of potential function $U(E(t))$. Bottom: Kinetic energy.

However, as in the friction compensated case, tracking performance improved when R was increased.

E. Effect of Nominal Speed: r

Finally, we investigate the effect of nominal speed on tracking performance. The nominal speed was varied by setting r in (36) to 1, 2, and 3 while R was kept at 100. Friction compensation was not used in these experiments. The relationship between the robustness bounds and the energy level in the system controlled

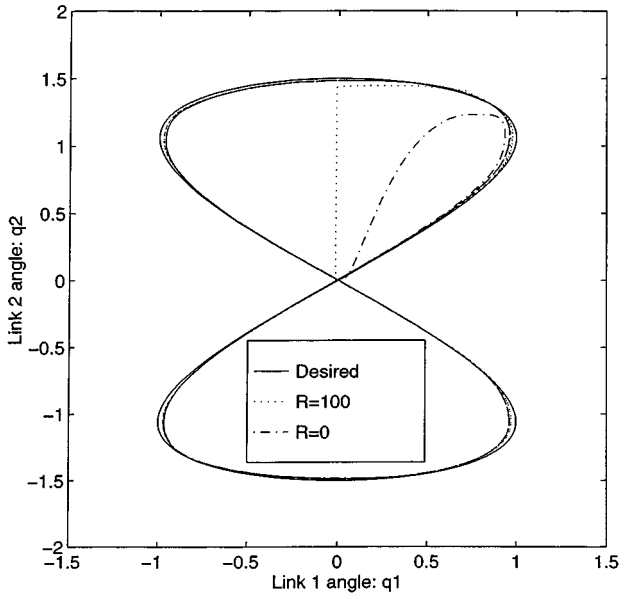

Fig. 7. Contour traced out by the manipulator with and without self-pacing when the initial position was not on the desired contour.

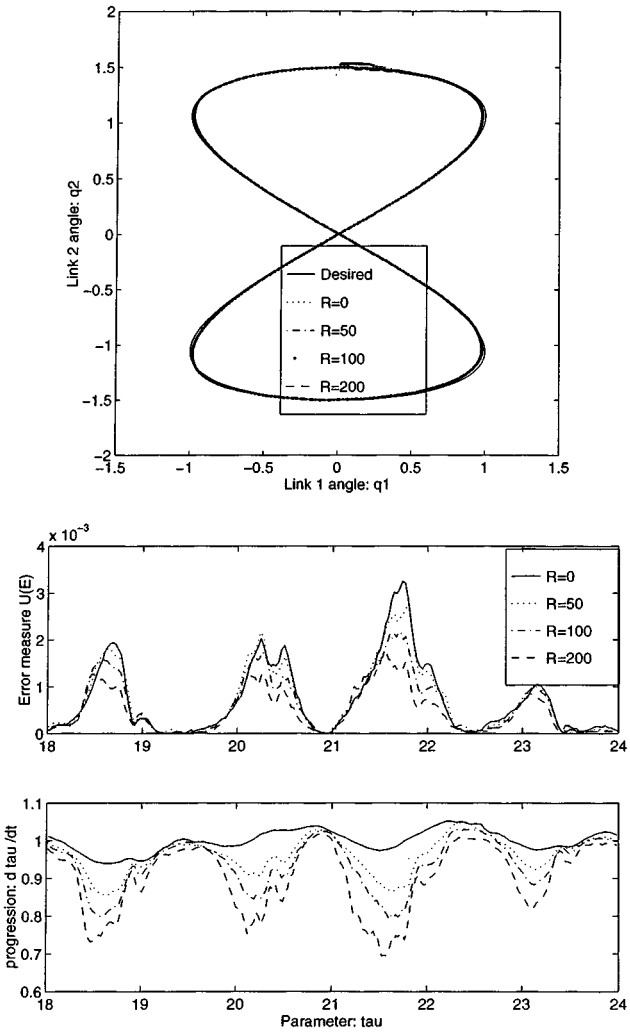

Fig. 8. Effects of different self-pacing parameter $R = 0$, 100, 200. Top: Contour traced. Middle: Value of the potential function $U(E)$ during one pass of the contour. Bottom: Rate of trajectory progression $\dot{\tau}$ during one pass of the contour.

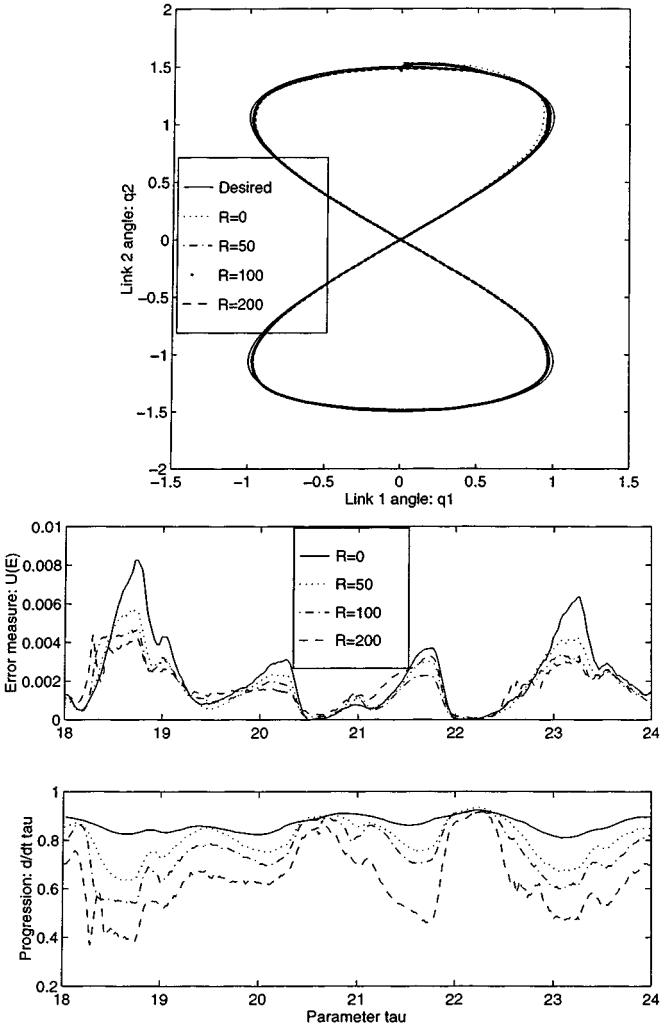

Fig. 9. Effects of different self-pacing parameter $R = 0$, 50, 100, 200 when friction compensation was removed. Top: Contour traced. Middle: Value of potential function during one pass of the contour. Bottom: Rate of trajectory progression $\dot{\tau}$ during one pass of the contour.

by the PVFC suggests that robustness to disturbances should improve at higher energy levels. Since the nominal speed determines the total energy level, it is expected that the tracking performance should improve as r increases. Fig. 10 shows that indeed the error measure $U(E)$ was significantly lower when r was increased from 1 to 2. The improvement, however, is not as notable when r was increased from 2 to 3.

VI. Conclusion

In this paper, the application of the PVFC methodology to contour following tasks for mechanical systems is discussed. The controller mimics the dynamics of an energy storage device and preserves the total energy of the system, rendering the closed-loop system passive when the environment force is considered as the input, the velocity as the output, and the environment power as the supply rate. In order to apply this control technique to contour following tasks, a velocity field must be designed which encodes the contour. A methodology for designing such a velocity field is presented when the configuration space

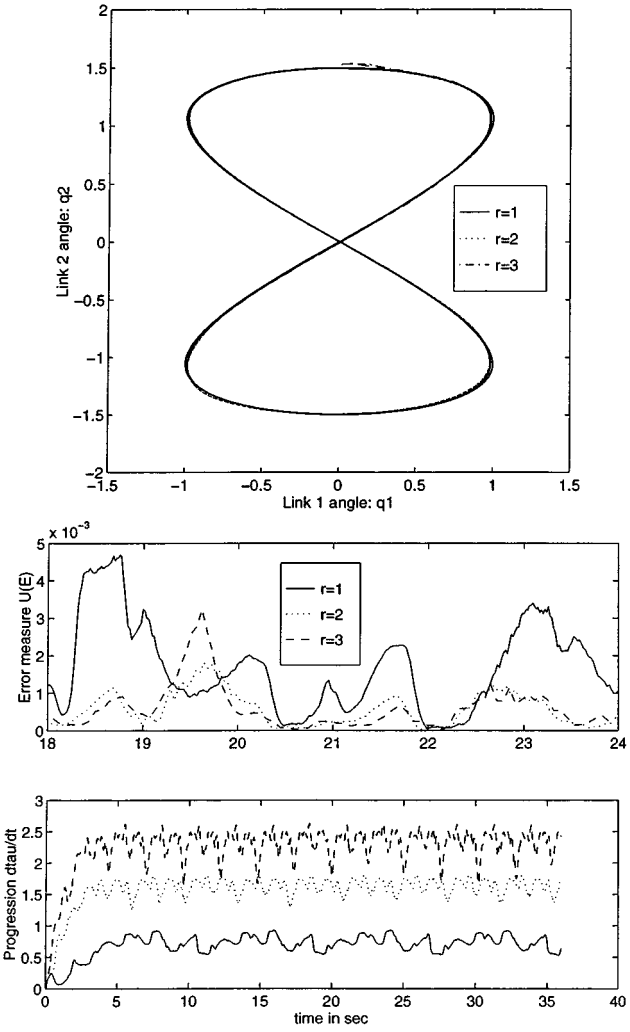

Fig. 10. Effects of different energy levels: $r = 1.0$, 2.0, 3.0 (without friction compensation). Top: Contour traced. Middle: Value of potential function. Bottom: Rate of trajectory progression $\dot{\tau}$.

of the system is a compact Lie group, and the contour is specified by a parameterized trajectory. The procedure involves suspending the contouring parameter by considering it as an extra coordinate, and then by designing a velocity field based on a gradient vector field of a navigation function. A simple *self-pacing* scheme which takes advantage of the flexibility of the timing along the contour to improve tracking performance is also proposed. The effectiveness of the contour following scheme is experimentally demonstrated on a two link direct drive robot following a Lissajous figure.

REFERENCES

[1] D. R. J. Chillingworth, J. E. Marsden, and Y. H. Wan, "Symmetry and bifurcation in three-dimensional elasticity, part I," *Arch. Rational Mech. Analy.*, vol. 80, no. 4, pp. 295–331, 1982.

[2] T. C. Chiu, "Coordination Control of Multiple Axes Mechanical System: Theory and Experiments," Ph.D. dissertation, Dept. of Mechanical Engineering, Univ. of California, Berkeley, CA, 1994.

[3] M. Hirsch, *Differential Topology: Graduate Text in Math*. New York: Springer-Verlag, 1976, vol. 33.

[4] D. E. Koditschek, "Total energy for mechanical control systems," in *Dynamics and Control of Multibody Systems*. ser. AMS series on Contemporary Mathematics, J. Marsden, P. S. Krishnaprasad, and J. Simo, Eds. Providence, RI: American Mathematical Society, 1989, vol. 97, pp. 131–157.

[5] P. Y. Li, "Self-Optimizing Control and Passive Velocity Field Control of Intelligent Machines," Ph.D., Dept. of Mechanical Engineering, University of California, Berkeley, CA, 1995.

[6] P. Y. Li and R. Horowitz, "Passive velocity field control of mechanical manipulators," *IEEE Trans. Robot. Automat.*, vol. 15, pp. 751–763, Apr. 1999.

[7] ——, "Passive velocity field control (PVFC) Part 1—Geometry and robustness," *IEEE Trans. Automat. Contr.*, vol. 46, pp. 1346–1359, Sept. 2001.

[8] R. Murray, Z. X. Li, and S. S. Sastry, *A Mathematical Introduction to Robotic Manipulation*. New York: CRC Press, 1994.

[9] E. Rimon and D. E. Koditschek, "The construction of analytic diffeomorphisms for exact robot navigation on star worlds," *Trans. Amer. Math. Soc.*, vol. 237, no. 1, pp. 71–116, Sept. 1991.

[10] ——, "Exact robot navigation using artifical potential functions," *IEEE Trans. Robot. Automat.*, vol. 8, no. 5, pp. 501–518, Oct. 1992.

[11] E. Tung, "Identification and Control of High-Speed Machine Tools," Ph.D., Dept. of Mechanical Engineering, Univ. of, Berkeley, CA, 1993.

Perry Y. Li (S'87–M'96) received the B.A.(Hons) and M.A. degrees in electrical and information sciences from Cambridge University, Cambridge, U.K., the M.S. degree in biomedical engineering from Boston University, Boston, MA, and the Ph.D. degree in mechanical engineering from the University of California, Berkeley, in 1987, 1990, 1990, and 1995, respectively.

He is currently Nelson Assistant Professor in Mechanical Engineering at the University of Minnesota, St. Paul. Prior to joining the University of Minnesota in 1997, he was a Researcher at Xerox Corporation, Webster, NY. His research interests are in dynamic systems and control as applied to fluid power systems, robotics, manufacturing, man–machine systems, transportation systems, and imaging and printing.

Dr. Li was awarded the 2000–2002 Japan/USA Symposium on Flexible Automation Young Investigator Award, and the Achievement and Special Recognition Awards from Xerox.

Roberto Horowitz (M'89) was born in Caracas, Venezuela, in 1955. He received the B.S. degree (with highest honors) and the Ph.D. degree in mechanical engineering from the University of California, Berkeley, in 1978 and 1983, respectively.

In 1982, he joined the Department of Mechanical Engineering, University of California, Berkeley, where he is currently a Professor. He teaches and conducts research in the areas of adaptive, learning, nonlinear, and optimal control, with applications to microelectromechanical systems (MEMS), computer disk file systems, robotics, mechatronics, and intelligent vehicle and highway systems (IVHS).

Dr. Horowitz received the 1984 IBM Young Faculty Development Award and the 1987 National Science Foundation Presidential Young Investigator Award. He is a member of ASME.